Simulation of Neptunium Extraction in an Advanced PUREX Process — Model Improvement

Hongyan Chen[a1], Robin J. Taylor[b], Megan Jobson[a], David A. Woodhead[b] , Colin Boxall[c] , Andrew J. Masters[a] , Scott Edwards[c]

a: School of Chemical Engineering and Analytical Science, The University of Manchester, Manchester, M13 9PL, UK

b: National Nuclear Laboratory, Central Laboratory, Sellafield, Seascale, Cumbria, CA20 1PG, UK

c: The Lloyd's Register Foundation Centre for Nuclear Engineering, Engineering Dept, Lancaster University, Lancaster LA1 4YR, UK

Routing neptunium to a single product in spent nuclear fuel reprocessing is a significant challenge. In this work, we have further improved the simulation of neptunium extraction in an advanced PUREX flowsheet by applying a revised model of the Np(V)-Np(VI) redox reaction kinetics, a new nitric acid radiolysis model and by evaluating various models for the nitrous acid distribution coefficient. The Np disproportionation reaction is shown to have a negligible effect. The models are validated against published 'cold test' experimental results; the 'hot test' simulation suggests high neptunium radiolysis could help to achieve high recoveries using this flowsheet.

Key words: neptunium, Advanced PUREX, flowsheet simulation, radiolysis, nitrous acid

1. Introduction

Nuclear energy plays an important role in the supply of sustainable and secure electricity. However, reducing the impact on the environment is a critical challenge in development of next generation nuclear reactors and the associated fuel cycles. The spent nuclear fuel, which is highly radioactive and toxic, must be treated carefully before disposal. Due to the complexity of the nuclear reactions, there

---

[1] Corresponding Author: hongyan.chen@manchester.ac.uk

are many fission products, as well as transuranic actinides, present in spent nuclear fuel. Among them, neptunium has been highlighted to be of potential environmental impact, at least under certain conditions, due to its long half-life, high mobility and radiotoxicity.[1] Therefore, there are potential benefits if neptunium (as well as other minor actinides) is removed from spent nuclear fuel before storage in a geological disposal facility.[2-5]

The PUREX process has been successfully applied in spent nuclear fuel processing since the 1950s.[6] However, this process generally focused on the separate recovery of plutonium and uranium. In the solvent extraction process, neptunium is commonly distributed between aqueous and organic streams in the first cycle of PUREX flowsheets and thus requires specific stages to purify products from neptunium contamination. Routing neptunium from spent nuclear fuel to a single product will, therefore, simplify the process and this can lead to overall reductions in the radioactive waste volumes and plant size. The preferred method is to adjust the operational parameters of the primary separation stage of the PUREX process to route neptunium with uranium and plutonium as part of an "advanced PUREX" process designed for future closed fuel cycles.[7,8] However, the neptunium reduction-oxidation reactions are complicated due to the dual role of HNO_2, which reduces Np (VI) to Np(V) but at low concentrations catalyses the oxidation of Np(V) and the extractabilities of Np(IV), Np(V) and Np(VI) are significantly different.[8-10] Therefore, it is not easy to fully recover neptunium in this advanced PUREX process.[11,12] Thus a mathematical model of the process, implemented as simulation code, is needed to predict the neptunium extraction behaviour and to guide experimental design and flowsheet operation.

In previous work,[13] a process model for the flowsheet simulation of an advanced PUREX process[11] was developed and implemented in gPROMS which is a software environment allowing users to build, validate and execute steady-state and dynamic process models.[14] In this simulation code, the choice of rate equations for neptunium redox reactions has an important effect on the outcome of the model. The main equilibrium reaction of neptunium in the nitric acid solution is expressed as:[15]

$$NpO_2^+ + 1.5H^+ + 0.5NO_3^- \rightleftharpoons NpO_2^{2+} + 0.5HNO_2 + 0.5H_2O \qquad (1)$$
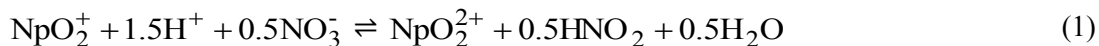
This reaction is one of the most complex reactions in spent nuclear fuel processing. Many studies of the reaction kinetics of this reaction are reported in literature.[15-20] However, these studies do not provide clear and consistent descriptions of the reaction rate.[21] Our previous simulation work adopted the kinetics of Koltunov[18] for this reaction. Based on the research of neptunium redox in aqueous-only phase and two-phase extractions,[11, 22] a revised description of neptunium kinetics is applied in this work to improve the simulation model.

During this reaction, the role of nitrous acid is important: it catalyses oxidation at low concentrations but acts as a reductant at high concentrations, reducing the Np(VI) to Np(V). Hence, predicting the distribution of nitrous acid in the advanced PUREX process simulation is a key requirement. In this work, a more accurate model of nitrous acid distribution coefficients (also known as distribution ratios) replaces the simple method of Uchiyama[23] used in our previous work.[13] Due to the influence of nitrous acid on the redox reaction, nitrous acid generated by radiolysis of nitric acid[24] also needs to be considered in flowsheet simulation of spent nuclear fuel re-processing. Therefore, a new model for calculating radiolytic nitrous acid production was integrated into the simulation of neptunium extraction. Finally, the effects of the disproportionation reaction of Np(V) were evaluated and are also reported in this paper.

2. Improvements in the neptunium extraction simulation

2.1 System overview

The Advanced PUREX flowsheet for neptunium co-extraction with uranium and plutonium reported by Taylor et al.[11] and modelled by ourselves[13] is illustrated in Figure 1. In this flowsheet, the neptunium in the aqueous feed F1 is assumed to be Np(V) because this is the most stable valence of neptunium in aqueous solution for up to 5M HNO_3 without nitrous acid present.[11, 25] As the distribution ratio of Np(VI) in the extraction agent, tributyl phosphate (TBP), is much larger than that of Np(V), this flowsheet was designed to oxidise most of the feed Np(V) to Np(VI) by nitric acid in

3

the presence of nitrous acid and then to extract Np(VI) by TBP. So, the aqueous feed A2 was designed to simulate radiolytically generated nitrous acid in the active feed to the cold test (using a surrogate solution without significant radiation power emission); this feed is not required in the subsequent 'hot test'(using real spent nuclear fuel) simulation. (Note that the nitrous acid in the aqueous feed F2 to the flowsheet is retained in the hot test simulation.)

2.2 Neptunium redox reaction model

In the previous work[13], we applied the reaction kinetic model of Koltunov [18] for the redox reaction equation (1). The current work replaces this kinetics model with expressions for the forward and reverse neptunium redox reaction kinetics as shown in Eq. (2) and (3) by Edwards et al.[26] which is based on the work of Moulin:[16]

$$v_F = -\frac{dC_{Np(V),aq}}{dt} = \frac{1.24 \times 10^8 e^{\left(-\frac{8540}{T+273}\right)} C_{H^+,aq} C_{NO_3^-,aq} C_{HNO_2,aq} C_{Np(V),aq}}{C_{HNO_2,aq} + C_{Np(V),aq}} \tag{2}$$

$$v_B = -\frac{dC_{Np(VI),aq}}{dt} = 1 \times 10^7 e^{\left(-\frac{6892}{T+273}\right)} C_{Np(VI),aq} \frac{\sqrt{C_{HNO_2,aq}}}{C_{H^+,aq}} \tag{3}$$

where T is temperature in °C, C is the concentration in mol·L^{-1}, v_F is the forward reaction rate and v_B is the reverse reaction rate. v_F and v_B are both in mol·L^{-1}·s^{-1}. The presence of the organic phase (TBP-diluent) can change the rate of the neptunium redox reaction. [16, 17, 27] Considering this effect, the rate constants and the activation energies in Eq. (2) and (3) have been regressed against our single-stage two-phase neptunium extraction experimental data.[11] The organic phase redox reaction kinetic model is the same as that used previously.[13]
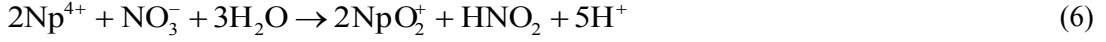
2.3 Disproportionation of neptunium (V)

The forward and reverse disproportionation reaction of Np(V) are expressed as Eq. (4) and Eq. (5), respectively: [28]

$$2NpO_2^+ + 4H^+ \rightarrow Np^{4+} + NpO_2^{2+} + 2H_2O \tag{4}$$

$$NpO_2^{2+} + Np^{4+} + 2H_2O \rightarrow 2NpO_2^+ + 4H^+ \tag{5}$$

Np(IV) can be oxidised by nitric acid according to the reaction [16]:

$$2Np^{4+} + NO_3^- + 3H_2O \rightarrow 2NpO_2^+ + HNO_2 + 5H^+ \tag{6}$$

The kinetics of these reactions have been investigated by several researchers.[16,28-32] Koltunov et al.[29] found that, in the aqueous phase, the rate of disproportionation of Np(V) is dependent on the concentration of Np(V) and the acidity:

$$-\frac{dC_{Np(V),aq}}{dt} = 2.67 \times 10^{-5} e^{-\frac{68700}{8.314}\left(\frac{1}{T+273}-\frac{1}{298}\right)} C_{Np(V),aq}^2 C_{H^+,aq}^2 \tag{7}$$

In the organic phase, the reaction kinetic model for this reaction given by Sarsfield et al. is:[31]

$$-\frac{dC_{Np(V),or}}{dt} = 0.74 e^{-\frac{93000}{8.314}\left(\frac{1}{T+273}-\frac{1}{298}\right)} C_{Np(V),or}^2 C_{HNO_3,or}^{1.21} C_{TBP.or}^{-4.35} \tag{8}$$

In the aqueous phase, Tachimori[33] (citing Rykov et al. [34]) proposed a reaction kinetic equation for the reproportionation reaction (Eq. (5)):

$$-\frac{dC_{Np(VI),aq}}{dt} = 4.17 \times 10^{-2} e^{-\frac{103000}{8.314}\left(\frac{1}{T+273}-\frac{1}{298}\right)} C_{Np(IV),aq} C_{Np(VI),aq} \left(2.16 + 12.5 C_{N,aq}\right) \tag{9}$$

where $C_{N,aq} = C_{H^+,aq} + C_{Np(V),aq} + 2\left(C_{U(VI),aq} + C_{Np(VI),aq}\right) + 4\left(C_{Pu(IV),aq} + C_{Np(IV),aq}\right)$ is the total concentration of nitrate in the aqueous phase.

In the organic phase, Wehrey et al.[32] showed that the reaction rate of the reproportionation reaction is given by:

$$-\frac{dC_{Np(VI),or}}{dt} = 3.4 \times 10^{-6} e^{-\frac{96000}{8.314}\left(\frac{1}{T+273}-\frac{1}{298}\right)} C_{Np(IV),or} C_{Np(VI),or} C_{HNO_3,or}^{-2} \tag{10}$$

The rate of Np(IV) oxidation by nitric acid in the aqueous phase is calculated by the kinetic model of Moulin: [16]

$$-\frac{dC_{Np(IV),aq}}{dt} = 7.1 \times 10^{-5} e^{-\frac{105000}{8.314}\left(\frac{1}{T+273}-\frac{1}{298}\right)} C_{Np(V),aq} C_{Np(IV),aq} C_{HNO_2,aq}^{-0.5} \tag{11}$$

Together with Eq. (2) and (3), Eq. (7-11) fully define the kinetics of redox reactions in the aqueous and organic phases in our experiments[11] and are applied in simulation in this work. Kinetic expressions similar to Eq.(7-11) were used by Tachimori[33, 35] but with different Np(V)-Np(VI) redox

reaction kinetics which was also derived from the work of Moulin. The main modification to the reaction models in this work is, for the first time, to use the Np(V)-Np(VI) redox reaction kinetics of Eq. (2) and (3) . Furthermore, the parameters of Eq. (2) and (3) were regressed against single-stage two-phase experimental data.

2.4 Distribution coefficients

This work extends previous work[13] improves the model for determining nitrous acid distribution coefficients and adds a distribution coefficient model for neptunium (IV). As before, the distribution coefficients of nitric acid and uranium (VI) are calculated using the SEPHIS model,[36] and distribution coefficients of neptunium (VI) are calculated using the model of Kolarik.[37] The distribution coefficient of neptunium (V) is set to 0.01, consistent with the approach of Tachimori in the EXTRA.M code.[35]

The distribution coefficient of neptunium (IV) is calculated based on the relationship of Rozen for distribution coefficients[38]:

$$D_{Np(IV)} = \begin{cases} \dfrac{D_{Pu(IV)}}{4}, & \text{if } C_{U(IV)} = 0 \\ \dfrac{D_{Pu(IV)}}{4.5}, & \text{if } C_{U(IV)} \neq 0 \end{cases} \qquad (12)$$

The distribution coefficients of plutonium (IV) are calculated by the SEPHIS method.[36] The mean absolute percentage error (MAPE) of this method when applied to the 266 experimental data points of Kolarik and Dressler [39] is about 40%. This agreement is better than that with the model of Kolarik[37] (MAPE: 50%) or of Tachimori[35] (MAPE > 100%).

Several reports present models for predicting the distribution of nitrous acid between the aqueous nitric acid solution and the TBP-diluent.[23, 35, 40 - 44] Figure 2 summarises the accuracy of these models with respect to the published experimental data[23, 44 - 49] listed in Table 1. Among those models, the method of Tachimori[35] has the lowest MAPE when nitric acid concentration is higher than 4 mol·L^{-1}.

As the advanced PUREX process operates at corresponding nitric acid concentrations, the method of Tachimori is applied in this work. This method is similar to that employed by Kolarik in the investigation of nitric acid and metal species in a nitric acid-TBP system[37] and is expressed in Eq. (13) to Eq. (16):[35]

$$D_{HNO2} = a_{93}C_{N,aq}^{a_{94}} \div (1 + a_{95}C_{N,aq}^{a_{96}} + a_{97}C_{HNO_2,aq}^{a_{98}} + a_{99}C_{6,aq}^{a_{100}} + a_{101}C_{4,aq}^{a_{102}} + a_{103}C_{H,aq}^{a_{104}}$$
$$+ a_{105}C_{N,aq}^{a_{106}}C_{HNO_2,aq} + a_{107}C_{N,aq}^{a_{108}}C_{6,aq} + a_{109}C_{N,aq}^{a_{110}}C_{4,aq} + a_{111}C_{N,aq}^{a_{112}}C_{H,aq}) \tag{13}$$

$$C_{6,aq} = C_{U(VI),aq} + C_{Np(VI),aq} + C_{Pu(VI),aq} \tag{14}$$

$$C_{4,aq} = C_{Np(IV),aq} + C_{Pu(IV),aq} \tag{15}$$

$$C_{N,aq} = C_{H^+,aq} + C_{Np(V),aq} + C_{Pu(V),aq} + 3C_{Pu(III),aq} + 2(C_{U(VI),aq} + C_{Np(VI),aq} + C_{Pu(VI),aq})$$
$$+ 4(C_{U(IV),aq} + C_{Np(IV),aq} + C_{Pu(IV),aq}) \tag{16}$$

a_{93} to a_{112} are regressed parameters. C_i is the concentration of species i. Concentrations are in mole·L^{-1} in Eq. (13) and (16) with the exception of $C_{6,aq}$ and $C_{4,aq}$ in Eq. (13), where the units are g·L^{-1}; in Eq. (14) and Eq. (15), all concentrations are in g·L^{-1}. The corresponding parameters were obtained from the literature[35] and are listed in Table 2.

2.5 Radiolytic yield of nitrous acid

A model based on G-values is usually used to calculate the radiolytic yield in a radiation environment, where the G-value for a radiolytic reaction generating a particular species is the number of molecules produced or destroyed per unit of radiation energy absorbed by the solution.[50] Here we consider only the radiolytic yield of nitrous acid by α, β and γ radiation. The radiolytic yield rate of HNO$_2$ due to absorbed irradiation power W (J·s^{-1}) can be calculated as follows:

$$\frac{dN_{HNO_2,aq}}{dt} = G_{\alpha,HNO_2,aq} \cdot W_{\alpha,abs,aq} + G_{\beta,HNO_2,aq} \cdot W_{\beta,abs,aq} + G_{\gamma,HNO_2,aq} \cdot W_{\gamma,abs,aq} \tag{17}$$

$$\frac{dN_{HNO_2,or}}{dt} = G_{\alpha,HNO_2,or} \cdot W_{\alpha,abs,or} + G_{\beta,HNO_2,or} \cdot W_{\beta,abs,or} + G_{\gamma,HNO_2,or} \cdot W_{\gamma,abs,or} \tag{18}$$

For α-radiation, the G-value is usually about three times larger than that for γ-radiation, while the *G*-value of β-radiation is similar to that obtained by γ-radiation. The *G*-value (mol·J^{-1}) for γ-radiation (simply expressed as G_{HNO2}) was obtained from the literature[21] and is given in Eq. (19) and Eq. (20).

$$G_{HNO_2,aq} = 1.94 \times 10^{-8} C_{HNO_3,aq} \tag{19}$$

$$G_{HNO_2,or} = -2.927 \times 10^{-7} \left(C_{HNO_3,or}\right)^2 + 6.241 \times 10^{-7} C_{HNO_3,or} + 1.507 \times 10^{-7} \tag{20}$$

The β and γ radiation powers are usually treated together, therefore:

$$\frac{dN_{HNO_2,aq}}{dt} = 3G_{HNO_2,aq} \cdot W_{\alpha,abs,aq} + G_{HNO_2,aq} \cdot W_{(\beta\&\gamma),abs,aq} \tag{21}$$

$$\frac{dN_{HNO_2,or}}{dt} = 3G_{HNO_2,or} \cdot W_{\alpha,abs,or} + G_{HNO_2,or} \cdot W_{(\beta\&\gamma),abs,or} \tag{22}$$

In spent nuclear fuel reprocessing, radiative power originates from radioactive isotopes in both aqueous and organic solutions. We can calculate the total emitted radiation power from the sum of the isotopes' specific output power P_i (per unit mass) and their amount in each phase. This calculation is given in Eq. (23), where m_i is the atomic weight of isotope i, N_i is the molar amount of i. Values for P_i for some isotopes are listed in Table 3. (Note that Table 3 does not distinguish between the specific output powers of β and γ) We assume the same absorbed power per unit volume in aqueous and organic phases. The absorbed radiation power of aqueous and organic solutions then can be calculated as in Eq. (24) and (25), where V_{aq} and V_{or} are the holdup volumes in the centrifugal contactor. (The volume of connections between two contactors is treated as negligible in the model).

$$W_{k,emit} = \sum \left(P_{k,i} \cdot m_i \cdot \left(N_{i,aq} + N_{i,or}\right)\right), \text{ where } k = \alpha \text{ or } (\beta \& \gamma) \tag{23}$$

$$W_{k,abs,aq} = W_{k,emit} \cdot \frac{V_{aq}}{V_{aq} + V_{or}}, \text{ where } k = \alpha \text{ or } (\beta \& \gamma) \tag{24}$$

$$W_{k,abs,or} = W_{k,emit} \cdot \frac{V_{or}}{V_{aq} + V_{or}}, \text{ where } k = \alpha \text{ or } (\beta \& \gamma) \tag{25}$$

3. Simulation results

3.1 Cold test simulation

3.1.1 Single-stage neptunium extraction simulation

The actual neptunium extraction experiments carried out in a single-stage centrifugal contactor[11] are depicted in Figure 3. The single-stage neptunium extraction simulations emulate these real experiments. In these single-stage experiments, the organic phase is passed through the contactor once while the aqueous phase is cycled via a reservoir.

 i. Neptunium redox reaction kinetics

Figure 4 shows the results of simulations applying the new redox reaction kinetics described above for the single-stage contactor experiments. In these simulations, the radiolysis reaction is included in the simulation model; nitrous acid distribution coefficients are calculated by Eq. (13-16); all the mass transfer coefficients are set to 2×10^{-5} m·s^{-1}. Other parameters and models are the same as in our previous work.[13] The results in Figure 4 show reasonable agreement with the experimental results[11]. Figure 5 compares simulation predictions applying revised (Moulin) kinetics and Koltunov kinetics, together with the above revisions to the model, to experimental results. The mean absolute error (MAE) is taken to be the average value of the absolute error over all sample points of an experiment.

 ii. Neptunium disproportionation reactions

In nitric acid solutions, the neptunium (V) disproportionation reaction rate increases as the acidity increases. [25, 28] The rate of this reaction is slow, due to the requirement to break Np-O bonds when reducing neptunium (V) (NpO_2^+) to neptunium (IV) (Np^{4+}). Therefore this reaction usually makes a negligible contribution to neptunium speciation in nitric acid.[21] However, the nitric acid concentration is around 5 mol·L^{-1} in the advanced PUREX process; therefore the simulation of the

single-stage experiments[11] was carried out with and without including the disproportionation reaction to check the effects of this reaction.

Figure 6 presents the deviation between simulation results and experimental results with and without considering disproportionation reactions. It may be seen that the disproportionation of neptunium (V) does not significantly change the simulation results. The concentration of neptunium (IV) is significantly lower than that of other neptunium valences in both phases – an example is shown in Figure 7. This low concentration means that the disproportionation of neptunium (V) occurs but its influence on neptunium extraction is negligible at the experimental conditions.

iii.   Effects of radiolysis reaction

Figure 8 summarises the deviation between simulation results and experimental results, with and without the radiolysis model. It may be seen that the results are very similar. This is not surprising as the simulated experiments were cold test experiments so the radiation power was negligible. Hence, the radiolysis of nitric acid in both phases is negligible in these simulations and integrating the radiolysis model does not change the cold test simulation results. The following section explores the potential impact of radiation on the process by considering radiolysis.

3.1.2 Flowsheet (multi-stage) simulation

i.   Flowsheet simulation with various redox kinetics

The model of Koltunov for neptunium oxidation kinetics[18] was used in our previous work.[13] The oxidation reaction rate can be calculated as given in Eq. (26):[51]

$$-\frac{dC_{\text{Np(V)},aq}}{dt} = 2.884 \times 10^{11} e^{-\frac{9222}{T}} C_{\text{Np(V)},aq} C_{\text{HNO}_2,aq}^{0.5} C_{\text{H}^+,aq}^{z} C_{\text{NO}_3^-,aq}^{0.5}$$
$$+ 5.405 \times 10^{12} e^{-\frac{10031}{T}} C_{\text{Np(V)},aq} C_{\text{HNO}_2,aq} C_{\text{H}^+,aq} \tag{26}$$

The value of the index z was 0.5 originally; it is found that, for nitrous acid concentrations around 10^{-3} mol$\cdot$L^{-1}, a value of $z = 2$ gives a better fit to experimental data.[51] This change in the value of z might be due to the accelerating effect of the organic phase on the neptunium redox reaction [16,17,27] or because the original z value was obtained at different experimental conditions to those studied here.

The results are presented in Figure 9; these show that simulation with the revised kinetic model based on parameters obtained from single-stage experiments gives the best simulation of experimental results from the neptunium extraction flowsheet test. Simulation with Koltunov kinetics with $z = 2$ also gives good agreement with experimental data in HA banks (High Active banks, stages 5 to 14 in Figure 1) but deviates from the experimental results in the HS bank (Hot Scrub bank, Stages 1 to 4 in Figure 1). Simulation with Koltunov kinetics with $z = 0.5$ are quite different to experimental results, especially in the HA banks. As can be seen in Figure 9, Eq. (2) and (3) provide a more realistic prediction than the kinetic model used by Tachimori.[33,35]

ii.   *Effect of nitrous acid distribution coefficients*

In our previous work,[13] the method of Uchiyama[23] was applied to predict nitrous acid distribution coefficients for the nitric acid / TBP-OK (odorless kerosene) system. Figure 10 presents two sets of simulation results for a multi-stage flowsheet, using nitrous acid distribution coefficient models based on the work of Uchiyama[23] and of Tachimori;[35] these results are compared with the experimental data.

Figure 10 shows that the HNO_2 concentration profile simulated using the distribution coefficient model of Tachimori is in better agreement with the experimental profile than the simulated profile generated using the method of Uchiyama. Note that concentrations on stages 9 to 14 are below detectable limits of the relevant instruments. Figure 11 shows the simulated nitrous acid concentration in the organic phase. Figure 10 also indicates that, with the method of Tachimori, the HNO_2 concentrations predicted in the aqueous phase are closer to experimental data than the HNO_2

concentration predicted using the method of Uchiyama. However, Figure 10 shows that in the HS bank, discrepancies between the simulation results and the experimental data are still significant. These discrepancies may also cause deviation between predicted and measured neptunium concentration profiles in the HS bank shown in logarithmic scale in Figure 12 and 13. Figure 12 and Figure 13 also suggest that although the two approaches predict different nitrous acid concentration profiles in HA banks (particularly in stage 6-14) , predicted neptunium concentration profiles are relatively similar; differences in predictions are relatively small and only occur in the HA2 and HA3 banks (stages 9 to 14). That different nitrous acid concentration profiles could correspond to rather similar Np profiles is unexpected based on an intuitive analysis of kinetic equations such as Eq.(5) and Eq.(28); this result implies that the neptunium concentration profiles are affected by phenomena other than the reaction kinetics, such as extraction equilibrium and mass transfer effects.

iii.   *Hot test simulation*

Using the model presented above and validated against the results of the single-stage contactor experiments and cold test flowsheet, a flowsheet for reprocessing spent fuel was designed by simulation (here referred to as the 'hot test' flowsheet). In the cold test flowsheet experiment, to replicate the radiolytic generation of nitrous acid in the extraction process, an extra flow of $NaNO_2$ (stream A2 in Figure 1) was added into centrifugal contactor stage 7. In the hot test flowsheet this A2 feed was removed; the nitrous acid content of the feed (F2) was maintained at the same level as in the cold test.

For the purpose of developing and demonstrating this radiation model within the overall flowsheet simulation, spent nuclear fuel of the composition given in Table 4 is assumed as the active feed. The specific output powers of the species based on a reference spent fuel (40 GWd per tonne, 5 year cooled) are listed in Table 3. Presently, during the simulation of the extraction process, the plutonium (IV) distribution coefficient is calculated by SEPHIS model,[36] while the fission products (FP) and all other isotopes including trivalent minor actinides (MA) are treated as non-extracting nitrates[52]. To simplify the calculations, it is also assumed that the average molecular weight of these non-extracting

nitrates is 100 g·mol^{-1} and that the nitrate salt formed with any of them is FPNO$_3$ or MANO$_3$. These assumptions would be refined in future work. Further work would also be needed to consider redox reactions of plutonium for hot test simulation.

Simulation results for the hot test are shown in Figures 14 and 15. Figure 14 shows that the γ-radiation output power is stronger in the HA banks of contactors than in the HS bank. This effect is due to the strong γ-radiation from fission products which are modelled as being inextractable into TBP and are hence routed to the aqueous raffinate. The γ-radiation output power in the HS bank is consequently only due to the extracted (organic phase) plutonium. The α-radiation output power changes less significantly than that of γ-radiation. This may be explained based on the understanding of the two main contributions to α-radiation: about half the contribution is from plutonium extracted from the aqueous to the organic phase by TBP and then enters the HS bank, and about half is related to inextractable minor actinides which remain in the aqueous phase and flow to the HA bank.

Figure 15a shows the simulation results for nitrous acid in both cold and hot tests. It may be seen that nitrous acid concentrations are higher in the HS and HA1 banks (stages 1-8) in the cold test than in the hot test; this result implies that the amount of NaNO$_2$ added in A2 in the cold test is greater than the radiolysis yield calculated for the hot test. In the HA2 and HA3 banks, the modelling results show the nitrous acid concentration in the hot test is higher than in the cold test, and that the nitrous acid concentration reduces slowly from stage 9 to stage 14. This concentration profile is the result of radiolytic generation of nitrous acid in those stages.

Although the concentrations of nitrous acid in the HA2 and HA3 banks in the hot test are higher than those in the cold test, the concentration of nitrous acid in both phases is still less than 0.1 mmol·L^{-1}. At these low nitrous acid concentrations, the reduction of Np(VI) to Np(V) by nitrous acid is negligible; instead, the nitrous acid mainly acts as a catalyst to accelerate the oxidation reaction of Np(V) to Np(VI) by nitric acid. As a result, the low concentration of nitrous acid in HA2 and HA3 banks can improve the oxidation of Np(V) and the extraction of neptunium in these banks, thus

reducing the leak of neptunium to the aqueous raffinate. Figure 15b shows that in stages 9 to 14, the aqueous phase neptunium concentration in the hot test is less than that in the cold test, while in the hot test the organic phase neptunium concentration is slightly higher than that in the cold test. The simulation of the hot test shows that the nitrous acid yield through radiolysis can improve the neptunium extraction in the advanced PUREX process and that 99 % of neptunium would still be routed to the organic product when radiolysis occurs.

4. Conclusions

This paper reports an extension to a previously published (open source) flowsheet simulation code designed to model neptunium extraction in an Advanced PUREX flowsheet.[11] The purpose of the modifications above are to improve simulation accuracy by applying a new neptunium redox reaction kinetic model, by modifying the nitrous acid distribution coefficient model and by integrating a model for predicting radiolytic nitrous acid generation into the flowsheet model. The effects of disproportionation of neptunium are also investigated and these were proved to be negligible.

Simulations of flowsheet performance with and without radiolytic nitrous acid generation (known as hot and cold tests, respectively) are presented. The results of the cold flowsheet simulation are in reasonable agreement with experimental test results[11] and the accuracy of simulation is shown to have improved. The hot test simulation results indicate the likely influences of radiolysis on neptunium extraction under radiation conditions that will be present when reprocessing spent nuclear fuel. The hot test simulation shows that, without extra $NaNO_2$ added to feeds, that the flowsheet used in the cold test should still reach about 99 % recovery for neptunium (for the reference fuel and activity used). This result is supported in part by results from the CEA (France) who obtained an improved percentage recovery of neptunium from ~90% in a cold test to >99% in a hot test when testing a similar flowsheet using pulsed columns as the contacting equipment in their *Atalante* facility.[53] CEA also used a specific nitrous acid feed in the cold test but omitted this feed and relied on radiolytic generation of nitrous acid in the hot test. Therefore, it appears that this flowsheet design

can be used as the basis for a future hot test of the primary extract-scrub section of an advanced PUREX process that uses centrifugal contactors for separations.

Acknowledgements

List of abbreviations and acronyms

Symbols	Unit	Definition
a		Distribution coefficients model parameter
C	$mol \cdot L^{-1}$ or $g \cdot L^{-1}$	Concentration
G	$mol \cdot J^{-1}$	G value
M	$g \cdot mol^{-1}$	Atomic weight
N	moles	Moles
P	$W \cdot g^{-1}$	Specific output power
V	L	Volume
W	Watt	Radiation power
v	$mol \cdot L^{-1} \cdot s^{-1}$	Reaction rate
t	s or minute	Time
T	°C	Temperature

Subscripts

aq	Aqueous phase
abs	Absorbed
emit	Emitted radiation
or	Organic phase
α	α irradiation
β	β irradiation
γ	γ irradiation

References

1. Magill, J.; Berthou, V.; Haas, D.; Galy, J.; Schenkel, R. Impact limits of portioning and transmutation scenarios on the radiotoxicity of actinides in radioactive waste. *Nuclear Energy*. 2003,42,263-277.

2. Koch, L. Minor actinide transmutation- a waste management option. *J. Less-Common Met*. 1986, 122, 371-382.

3. Poinssot, C.; Boullis, B. Actinide recycling within closed fuel cycles. *Nuclear Eng. Int*. 2012, 57, 670, 17-21.

4. Abderrahim, H. A.; Paillère, H. *Strategic Research Agenda*, sustainable nuclear energy technology platform, Available at: http://www.snetp.eu/wp-content/uploads/2014/05/sar2009.pdf. [accessed 19 October 2015]

5. McCarthy, K. A. *Nuclear Fuel Cycle Transition Scenario Studies*. Nuclear Energy Agency, Organisation for Economic Cooperation and Development: Paris: 2009.

6. Irish, E. R.; Reas, W. H. *The PUREX process--A Solvent Extraction Reprocessing Method for Irradiated Uranium*. HW-49483A, Hanford Atomic Products Operation: Richland, Washington, USA, April, 1957.

7. Herbst, R. S.; Baron, P. Standard and advanced separation: PUREX processes for nuclear. In *Advanced Separation Techniques for Nuclear Fuel Reprocessing and Radioactive Waste Treatment*; K. L. Nash; G. J. Lumetta, Eds.; Woodhouse Publishing Ltd.: Oxford; 2011.

8. Taylor, R. J.; Denniss, I. S,; Wallwork, A. L. Neptunium control in an advanced PUREX process. *Nuclear Energy*. 1997, 36, 39-46.

9. Drake, V. A. Extraction chemistry of neptunium. In *Science and Technology of Tributyl Phosphate, Vol. III*; W. W. Schulz, et al., Eds; CRC Press: Boca Raton, FL; 1990.

10. Yoshida, Z.; Johnson, S. G.; Kimura, T.; Krsul, J. R. Neptunium. In *The Chemistry of the Actinide and Transactinide Elements*; L. R. Morss, et al., Eds.; Springer: Netherlands; 2011.

11. Taylor, R. J.; Gregson, C. R.; Carrott, M. J.; Mason, C.; Sarsfield, M. J. Progress towards the full recovery of neptunium in an Advanced PUREX process. *Solvent Ext. Ion Exch*. 2013, 31(4), 442-462.

12. Lecomte, M. E., Ed. *Treatment and Recycling of Spent Nuclear Fuel: Actinide Partitioning - Application to Waste Management*. CEA Saclay: Paris; 2008.

13. Chen, H.; Taylor, R. J.; Jobson, M.; Woodhead, D. A.; Masters, A.J. Development and validation of a flowsheet simulation model for neptunium extraction in an advanced PUREX process. *Solvent Ext. Ion Exch*. 2016, 34(4), 297-321.

14. Process Systems Enterprise. gPROMS Model Builder ©, Available at www.psenterprise.com, 1997-2015.

15. Siddall, T. H.; Dukes, E. K. Kinetics of HNO_2 catalyzed oxidation of neptunium(V) by aqueous solutions of nitric acid. *J. Am. chem. Soc.* 1959, 81(4), 790-794.

16. Moulin, J. P. *Kinetics of Redox Reactions of Neptunium in Nitric Acid: Oxidation of Neptunium (IV) into Neptunium(V) and Oxidation of Neptunium (V) into Neptunium (VI) by Nitric Acid, Catalyzed by Nitrous acid.* CEA-R-4912, L'Universite Pierre et Marie Curie & Commissariat a I'Energie Atomique: Fontenay-aux-Roses, France, 1978.

17. Swanson, J. L. *Oxidation of Neptunium (V) in Nitric Acid Solution: Laboratory Study of Rate Accelerating Materials (RAM)*. BNWL-1017, Battelle Memorial Institute - Pacific Northwest Laboratory: Richland, Washington, USA, April, 1969.

18. Koltunov, V.S. *Kinetika reaktsii aktinoidov (Kinetics of Actinide Reactions)*. Atomizdat: Moscow; 1974.

19. Tochiyama, O.; Nakamura, Y.; Hirota, M.; Inoue, Y. Kinetics of nitrous acid-catalyzed oxidation of neptunium in nitric acid-TBP extraction system. *J. Nuclear Sci. Technol.* 1995, 32(2), 118-124.

20. Gourisse, D. Oxidation du neptunium (V) par les solutions aqueous d'acide nitrique en presence d'acide nitreux. *J. Inorg. Nucl. Chem*. 1971, 33, 831-837.

21. Precek, M. *The Kinetic and Radiolytic Aspects of Control of the Redox Speciation of Neptunium in Solutions of Nitric Acid*. Oregon State University: Corvallis, Oregon; 2012.

22. Gregson, C.; Boxall, C.; Carrott, M.; Edwards, S.; Sarsfield, M.; Taylor, R.; Woodhead, D. Neptunium (V) oxidation by nitrous acid in nitric acid. *Procedia Chem*. 2012, 7, 398-403.

23. Uchiyama, G.; Hotoku, S.; Fujine, S. Distribution of nitrous acid between tri-n-butyl phosphate/n-dodecane and nitric acid. *Solvent Extr. Ion Exch*. 1998, 16(5), 1177-1190.

24. Kazanjian, A. R.; Miner, F. J.; Brown, A. K.; Hagan, P. G.; Berry, J. W. Radiolysis of nitric acid solution: L.E.T. effects. *Transactions of the Faraday Society*. 1970, 66, 2192-2198.

25. Shilov, V. P.; Gogolev, A. V.; Fedoseev, A. M. Speciation, stability, and reactions of Np(III–VII) in aqueous solutions. *Radiochemistry*. 2012, 54, 212-217.

26. Edwards, S. E.; Boxall, C.; Taylor, R. J.; Woodhead, D. A. *Solvent Ext. Ion Exch*., 2017, in preparation.

27. Mincher, B. J.; Precek, M.; Paulenova, A. The redox chemistry of neptunium in γ-irradiated aqueous nitric acid in the presence of an organic phase. *J. Radioanal Nucl. Chem.* 2016, 308, 1005-1009.

28. Escure, H. *Contribution a L'etude de la Dismutation du Neptunium Pentavalent en Solution Acide*. CEA-R-4574, Centre d'Etudes Nucléaires de Fontenay-aux-Roses: Fontenay-aux-Roses, France, October, 1974

29. Koltunov, V. S.; Tikhonov, M. F. Kinetics of the disproportionation of neptunium(V) in a nitric acid solution. *Radiokhimiya*. 1975, 17(4), 560-563.

30. Hindman, J. C.; Sullivan, J. C.; Cohen, D. Kinetics of reactions between neptunium ions. The Np(IV)-Np(VI) reaction in perchlorate solution. *J. Am. Chem. Soc*. 1954, 76(12), 3278-3280.

31. Sarsfield, M. J.; Taylor, R. T.; Maher, C. J. Neptunium (V) disproportonation and cation-cation interactions in TBP-kerosene solvent. *Radiochim. Acta.* 2007, 95, 677-682.

32. Wehrey, F.; Guillaume, B. Kinetics of the neptunium(IV)-neptunium(VI) reaction and of the oxidation of neptunium (V) by nitric acid in Tributylphosphate -n- dodecane solutions. *Radiochim. Acta.* 1989, 46, 95-100.

33. Tachimori, S. Numerical simulation for chemical reactions of actinide elements in aqueous nitric acid solution. *J. Nucl. Sci. Technol*. 1991, 28(3), 218-227.

34. Rykov, A.G. and Yakovlev, G. N. Redox reactions of the actinides. II. Kinetics for the reaction between neptunium(IV) and neptunium(VI) in nitrate solutions. *Radiokhimiya.* 1966, 8(1), 27-32.

35. Tachimori, S. *EXTRA.M: A Computer Code System for Analysis of the Purex Process with Mixer Settlers for Reprocessing*. JAERI 1331, Japan Atomic Energy Research Institute: Tokai-mura, Naka-gun, Ibaraki-ken, Japan, 1993.

36. Jubin, R. T. *A Modified Mathematical Model for Calculating Distribution Coefficients for U (VI) , Pu (IV) , and Nitric Acid in the Uranyl Nitrate-plutonium (IV) Nitrate-nitric Acid-water/tributyl Phosphate System*. ORNL/TM-7217, Oak Ridge National Laboratory: Oak Ridge, Tennessee, USA, April, 1980.

37. Kolarik, Z,; Petrich, G. A mathematic model of distribution equilibria in the extraction of U(VI), U(IV), Pu(IV), Np(VI), Np(IV), and nitric acid by 30% tributyl phosphate (TBP) in aliphatic diluents. *Ber.Bunsenges. Phys. Chem.* 1979, 83, 1110-1113.

38. Rozen, A. M.; Andrutskii, L. G.; Vlasov, V. S. Improved mathematical models of actinide extraction by 30% solutions of the tri-n-butylphosphate in diluents. *Atomnaya Energiya*. 1987, 62(4), 227-231.

39. Kolarik, Z.; Dressler, P. *PUREX Process Related Distribution Data on Neptunium (IV,VI)*. KfK-4667, Karlsruhe, Germany, January, 1990.

40. Nabeshima, M. Prediction of mass transfer and heat evolution of PUREX pulsed columns by the DYNAC computer model. *Nuclear Technology*. 1991, 95, 33-43.

41. Hotoku, S.; Kihara, T.; Uchiyama, G.; Fujine, S.; Maeda, M. *Distribution Equilibrium of Nitrous Acid in Reprocessing Solution*. JAERI-M 93-095, Japan Atomic Energy Research Institute: Tokai-mura, Naka-gun, Ibaraki-ken, Japan, 1993.

42. Tsubata, Y.; Asakura, T.; Morita, Y. *Development of a Computer Code, PARC, for Simulation of Liquid-liquid Extraction Process in Reprocessing*. JAEA-Data/Code 2008-010, Japan Atomic Energy Agency: Tokai-mura, Naka-gun, Ibaraki-ken, Japan, 2008.

43. Kumar, S.; Koganti, S. Modelling of distribution coefficients of nitrous acid in 15-30 vol.% TBP n-dodecane -nitric acid system. *Indian Journal of Chemical Technology*. 2000, 7, 336-337.

44. Zhu, L.; Chen, Y.; Tang, H.; He, H. Distribution coefficient of nitrous acid and its computer simulation. *Journal of Nuclear and Radiochemistry*. 2014, 36(4), 229-234.

45. French, E. S. *Distribution of Nitrous Acid Between Mainly 30%TBP/OK and Aqueous Nitric Acid*. Chem Group Memo 176, BNFL R&D Department: Cumbria, UK, Decomber, 1988.

46. Jenkins, L. *Distribution of Nitrous Acid Between 30%TBP/OK and Aqueous Nitric Acid*. Chem Group Memo 182, BNFL R & D Department: Cumbria, UK, April, 1989.

47. Jenkins, L. *Distribution of Nitrous Acid Between 30%TBP/OK and Aqueous Nitric Acid in the Presence of Uranium(VI)*. Chem Group Memo 183, BNFL R & D Department: Cumbria, UK, April, 1989.

48. Burger, L. L.; Money, M. D. *Nitrous Acid Behavior in PUREX Systems*. HW-60278, General Electric: Richland, Washington, USA, May, 1959.

49. Biddle, P.; Miles, J. H. Rate of reaction of nitrous acid with hydrazine and with sulphamic acid. *J. Inorg. Nucl. Chem.* 1968, 30, 1291-1297.

50. Loveland, W.; Morrissey, D. J.; Seaborg, G. T. *Modern Nuclear Chemistry*. John Wiley & Sons, Inc.: Hoboken, New Jersey; 2006.

51. Birkett, J. E.; Carrott, M. J.; Fox, O. D.; Jones, C. J.; Maher, C. J.; Roube, C. V.; Taylor, R. J.; Woodhead, D. A. Controlling neptunium and plutonium within single cycle solvent extraction for advanced fuel cycles. *J. Nucl. Sci. Technol*. 2007, 44(3), 337-343.

52. Nakahara, M.; Nakajima, Y.; Koizumi, T. Extraction behavior of fission products with tri-n-butyl phosphate by countercurrent multistage extraction in a uranium, plutonium,and neptunium co-recovery system. *Industrial & Engineering Chemistry Research*. 2012, 51, 13245−13250.

53. Dinh, B.; Mosiy, P.; Baron, P.; Calor, J. N.; Espinoux, D.; Lorrain, B; Benchikouhne-Ranchoux, M. Modified PUREX first cycle extraction for neptunium recovery, In *Solvent Extraction: Fundamentals to Industrial Applications*; B. A. Moyer, Ed.; Proceedings ISEC 2008 International Solvent Extraction Conference; 2008, 581-586.

Tables:

Table 1 Experimental nitrous acid distribution coefficients data

Table 2 Parameters of equation (13) [35]

Table 3 Specific output powers

Table 4 Hot test feeds

Table 1 Experimental nitrous acid distribution coefficients data

Author	$[HNO_3]_{aq}$, mol·L^{-1}	$[U]_{aq}$, g·L^{-1}	$[U]_{or}$, g·L^{-1}	$[HNO_2]_{aq}$, mmol·L^{-1}	Temperature, °C	No. of data points
Uchiyama, G. , et al. [23]	0-4	0-14.5	0-80	1.4	25	11
French, E.S. [45]	0.1-4	none	none	2-71	22	43
Jenkins, L., [46,47]	0.1-2	0-110	0-91.2	0.6-92.3	22-35	186
Zhu, L., et al. [44]	0.433-4.355	none	none	0.165-4.174	25	20
Burger, L.L and Money M.D. [48]	0-8		0-116	<10	25-50	22
Biddle, P. and Miles, J.H. [49]	0.95-2.91		0-71.4	2.4-12.5	20	11

Table 2 Parameters of equation (13) [35]

a_{93}	28.526	a_{94}	0.01869	a_{95}	0.11958	a_{96}	1.8174	a_{97}	0.009986
a_{98}	4.5326	a_{99}	0.9194	a_{100}	0.000507	a_{101}	0	a_{102}	1
a_{103}	0.24621	a_{104}	1.0622	a_{105}	0.5977	a_{106}	3	a_{107}	0.02016
a_{108}	2.6322	a_{109}	0	a_{110}	1	a_{111}	0.2962	a_{112}	0.5822

Table 3 Specific output powers

Isotope	Specific output power (W/g), α-radiation	Specific output power (W/g), β- and γ-radiation
^{234}U	0.000179023	
^{235}U	5.99346×10^{-8}	
^{236}U	1.75418×10^{-6}	
^{238}U	8.51157×10^{-9}	
^{237}Np	0.000704728	
^{238}Pu	0.56771	
^{239}Pu	0.0019283	
^{240}Pu	0.00706947	
^{241}Pu		0.00327218
^{242}Pu	0.000116829	
Reference spent fuel Pu (40 GWd/te, 5 year cooled)	0.01207	
Reference spent fuel (40 GWd/te, 5 year cooled)	2.53×10^{-4}	0.001929
Total U*	5.77×10^{-8}	0
Total Pu	0.01207	6×10^{-4}**
FP and in-extractable minor actinides***	0.01317	0.1923

*calculated based on the fuel of 98%U, 1%Pu and 1%FPs, the uranium isotope is 0.022% ^{234}U, 1.09% ^{235}U, 0.53% ^{236}U, and 98.35% ^{238}U;

**suppose the radiation power of plutonium is about 95% α-radiation and 5% β- and γ-radiation.

*** all other isotopes' output radiation powers are counted in this item

Table 4 Hot test feeds

	A1	F1	F2	A2	S1
U(VI), $g \cdot L^{-1}$	0	277	0	0	0
Pu(IV), $g \cdot L^{-1}$	0	2.77	0	0	0
Np(V), $mg \cdot L^{-1}$	0	166	0	0	0
Np(VI), $mg \cdot L^{-1}$	0	0	0	0	0
FPs, $mg \cdot L^{-1}$	0	2.77	0	0	0
HNO_2, $mol \cdot L^{-1}$	0	0	0.073	0	0
HNO_3, $mol \cdot L^{-1}$	4.5	5	0	0	0.05
TBP, %					30
Flow rate ($mL \cdot min^{-1}$)	0.45	0.9	0.1	0	3

Table 4 Hot test feeds